LCLS UNDULATOR COMMISSIONING, ALIGNMENT, AND PERFORMANCE *

H.-D. Nuhn# for the LCLS Commissioning Team,
SLAC National Accelerator Laboratory, Stanford, CA 94309, U.S.A.

Abstract

The LCLS x-ray FEL has recently achieved its 1.5-Angstrom lasing and saturation goals upon first trial. This was achieved as a result of a thorough pre-beam checkout, both traditional and beam-based component alignment techniques, and high electron beam brightness. The x-ray FEL process demands very tight tolerances on the straightness of the electron beam trajectory (<5 μm) through the LCLS undulator system. Tight, but less stringent tolerances of ~100 μm rms were met for the transverse placement of the individual undulator segments with respect to the beam axis. The tolerances for electron beam straightness can only be met through a beam-based alignment (BBA) method, which is implemented using large electron energy variations and sub-micron resolution cavity beam position monitors (BPM), with precise conventional alignment used to set the starting conditions. Precision-fiducialization of components mounted on remotely adjustable girders, and special beam-finder wires (BFW) at each girder have been used to meet these challenging alignment tolerances. Longer-term girder movement due to ground motion and temperature changes are being monitored, continuously, by a unique stretched wire and hydrostatic level Alignment Diagnostics System (ADS).

INTRODUCTION

The undulator system for the Linac Coherent Light Source (LCLS), in operation at the SLAC National Accelerator Laboratory (SLAC NAL), is comprised of 33 mechanically identical 3.4-m-long undulator segments, separated from each other by short and long breaks. A detailed description of the undulators system with alignment strategy and tolerances is given in [1]. This paper reports experiences with implementing these concepts through commissioning and first lasing.

UNDULATOR SEGMENT TUNING

The Undulator Segments [2] are fixed-gap permanent magnet planar undulators with a period length of 3 cm and a nominal undulator parameter of K_{eff} = 3.5, and are mounted inside a 3.4-m-long Ti strongback. The undulator gap is arranged such that the electron wiggle motion is in the horizontal plane. The upper and lower pole face planes are canted with respect to each other by an angle of about 5.5-mrad, which makes their K_{eff} values dependent on the electron beam's horizontal position inside the undulator (in addition to its dependence on the vertical position for the regular planar undulator).

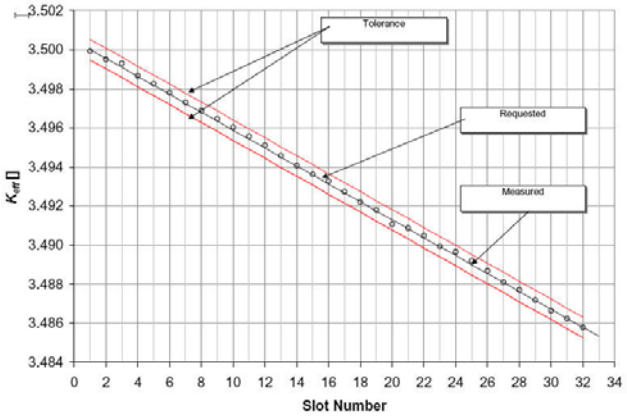

Figure 1: Goal and measured values of K_{eff} for the LCLS Undulator Segments.

Each undulator has been tuned [3] to a different effective K_{eff} value (see tapering, below) to compensate for energy losses during the radiation process and to optimize the SASE process. (see Fig. 1) The magnetic axis, i.e., the ideal average beam trajectory through the undulator segment, has been determined during the tuning of the device and fiducialized to tooling balls on the device body. Fig. 2 shows the difference between the measured and goal K_{eff} values, which are all well within tolerance.

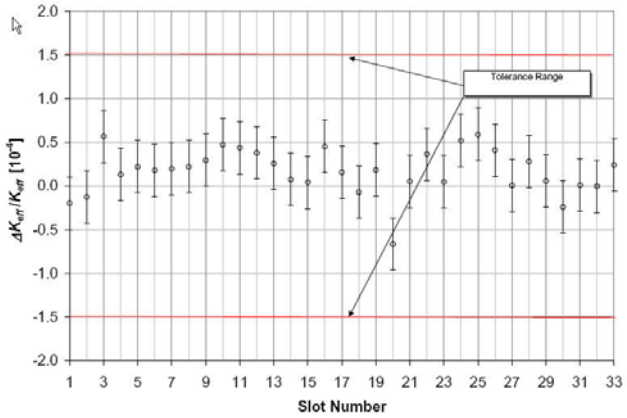

Figure 2: Relative deviation of the on-axis K_{eff} values from the goal as measured by Hall probes in the Magnet Measurement Facility (MMF).

Fig. 3 shows the rms phase error (phase shake) between the electron beam and the x-ray wave along each Undulator Segment as well as the total phase mismatch over an Undulator Segment Cell (cell match) , i.e., the

* Work by U.S. Department of Energy contract DE-AC02-76SF00515
# nuhn@slac.stanford.edu

fixed distance over which the phase slippage should be 113 x-ray wavelengths. The measured values of both the phase shake and the cell match are well within the tolerance of 10 degree of x-ray phase.

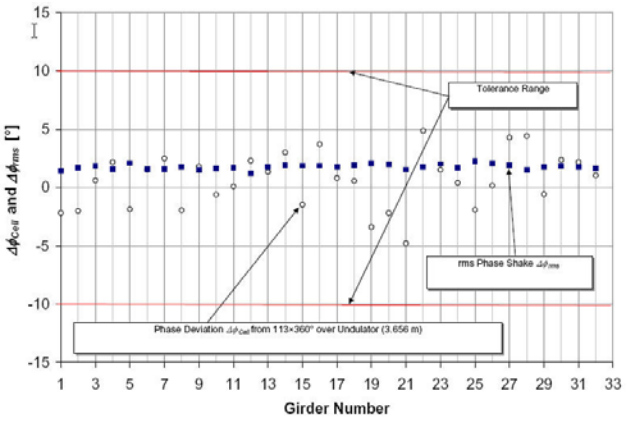

Figure 3: RMS phase error (phase shake) and accumulative phase error across each undulator cell as measured using Hall probes in the MMF.

PRE-BEAM CHECKOUT

After all components of the undulator system (except the Undulator Segments themselves) had been installed in the Undulator Hall, an extensive pre-beam checkout procedure (204 pages) was carried out. For each girder the functionality of 13 different subsystems was checked through the EPICS control system using the final operational control screens. Those 13 subsystems included: Beam Finder Wire (BFW), Beam Loss Monitor (BLM), cam system components, linear potentiometers (LP), girder motion, horizontal slides, quadrupole, horizontal and vertical correctors, RFBPM, temperature sensors (RTDs), wire position monitors (WPM), and hydrostatic leveling system (HLS) components. Problems with either the components themselves or with the control system functionality were corrected as they were found.

GIRDER POSITION MONITORING

The alignment of the girders is continuously monitored at sub-micron resolution by the Alignment Diagnostics System (ADS), which is a combination of a Wire Position Monitor (WPM) system and a Hydrostatic Leveling System (HLS), both permanently installed.

There are four sensors for each of the two subsystems mounted on each girder, two each close to either end of the Undulator Segment. The HLS is most sensitive to vertical positioning, while the WPM is best for horizontal positioning.

Figs. 4 and 5 give an example of both the 100 nm resolution of the system as well as the stability of the girder components as measured by the ADS.

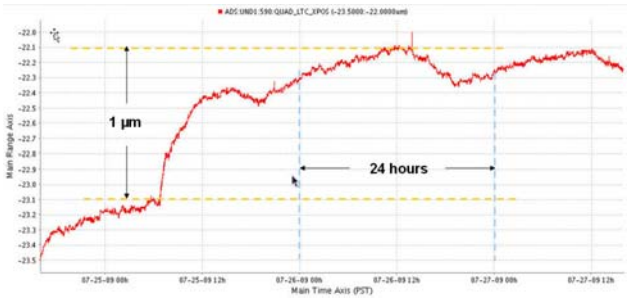

Figure 4: Horizontal position of quadrupole QU15 as monitored by the ADS over a period of about 3 days while no cam motion or segment movement occurred.

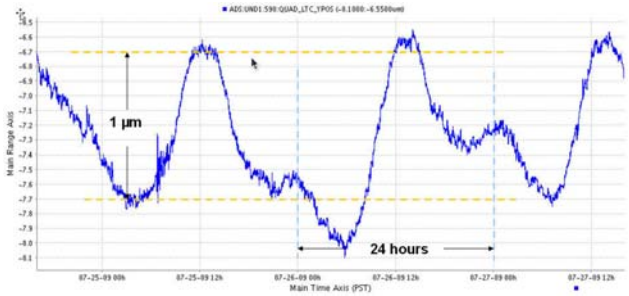

Figure 5: Vertical position of quadrupole QU15 as monitored by the ADS over a period of about 3 days while no cam motion or segment movement occurred. A diurnal cycle at about ±0.5 µm can be identified.

TUNNEL TEMPERATURE

On every girder, temperature is monitored at 12 control points, including three positions on the undulator body, itself. Those three temperature sensors are calibrated and are used to adjust the temperature dependent undulator parameter, *K*.

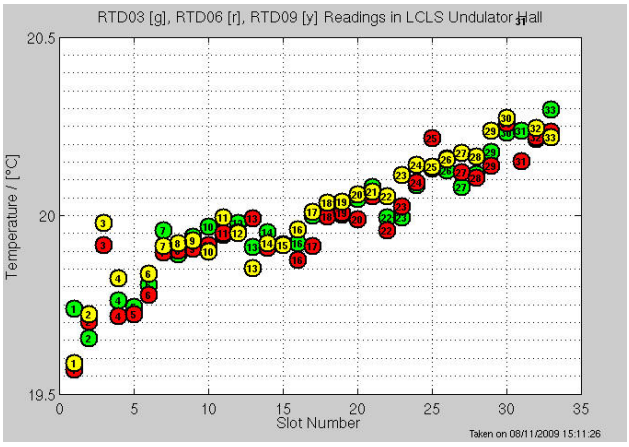

Figure 6: Readings of all 99 calibrated temperature sensors (RTDs) mounted at the upstream (green), center (yellow) and downstream (red) position of each of the 33 Undulator Segments.

Fig. 6 shows an example of the readings of the RTDs that are used to keep the undulator *K* values constant under temperature variation. The vertical range of the plot

is identical to the temperature tolerance for the Undulator Hall. The rms spread is of order 100 mK. The linear increase in temperature along the girders is due to the design of the air handler system (HVAC), which controls the temperature of the LCLS undulator tunnel by a constantly flowing, thermally regulated, air stream [4]. The air enters upstream of the first girder and is blown through the 170-m-long tunnel in downstream direction. Temperature monitoring is done at the entrance point. As the air travels through the tunnel it picks up heat from the undulator equipment at a rate of about 60 W/m. The system keeps the air temperature in the range of 19.5° C-20.5° C at all times along the entire undulator system. The undulator *K* value has been measured to change by 0.015% over a temperature range of 0.28° C.

Fig. 7 shows the readings of one temperature sensor over about 15 days. During operation, a tiny diurnal cycle, less than ±25 mK is detectable. During access, the tunnel lighting is turned on and the tunnel and Undulator Segment temperatures start to rise. Presently, the change in light status is part of the PPS. A change of this procedure is under consideration.

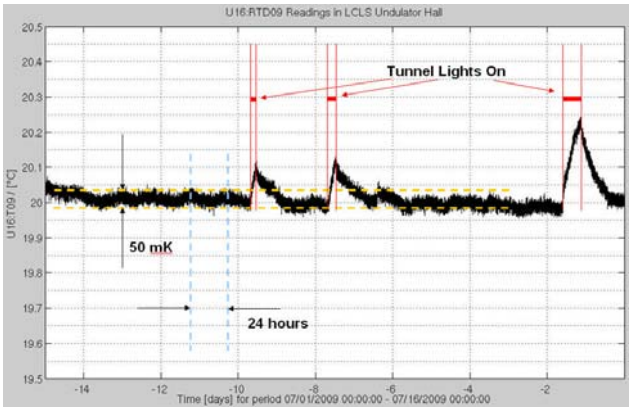

Figure 7: History of the readings of the temperature censor attached to the center of Undulator Segment 16.

The excellent temperature stability of the LCLS undulator tunnel during periods of operation is an important contributor of the observed system stability.

FIRST BEAM

Before the first electron beam was sent through the undulator vacuum pipe, the girder positions had been corrected in *x* and *y* using the cam movers; mostly to align the beam pipes and the quadrupoles as close to a straight line as possible but also to use the off-axis quadrupole fields to compensate for the environmental tunnel field (modified earth magnetic field and fields from various tunnel components). Both corrections were based on measurements provided by the Metrology group.

The first beam shot did not need any alignment correction to pass through undulator beam pipe (5×12 mm cross-section; 132 m long) to the main dump. The maximum trajectory error was only about 1 mm.

BEAM-BASED FIELD INTERALS

During undulator tuning in the Magnet Measurement Facility (MMF), the horizontal and vertical field integrals of all undulators were measured along the undulator axis at different *x* locations using a long coil arrangement. These field integrals all came out well within the tolerance of ±40 μTm. Due to the high resolution of the Cavity Beam Position Monitors (RFBPMs), it was possible to use the beam to verify the relative *x* dependence of the first field integrals. The absolute amplitudes of the field integrals are not accessible by this beam based method, which fits the model to the difference of the trajectory through the undulator at location *x* compared to location *x* = 0. The fit assumes a kick in the longitudinal center of the undulator.

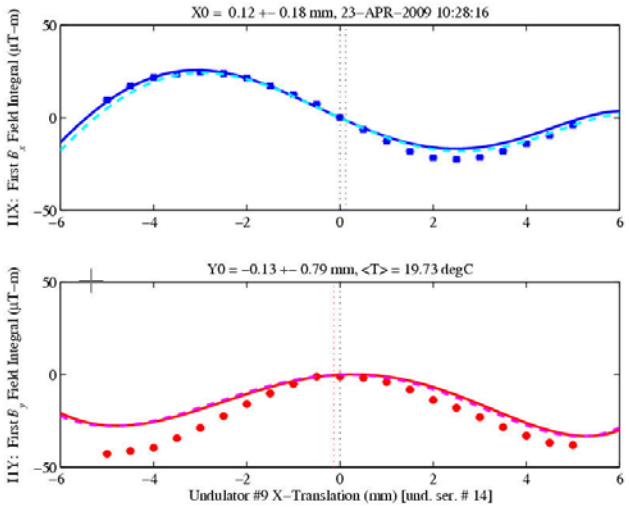

Figure 8: Horizontal and vertical first field integrals along the magnetic axis of undulator U09 measured both long-coil based (solid line) and beam-based. The offset of beam-based measurements has been adjusted to agree with the long-coil based method at *x* = 0.

The fit results for these kicks are converted to field integrals to a kick angle resolution of 20 nrad and included in Fig. 8. As the figure illustrates, the functional dependence, which is different and characteristic for each undulator is fairly well confirmed by the beam based method.

FIRST UNDULATOR *K* MEASUREMENT

The strength (*K* values) of the individual undulators can be confirmed with the beam using the K-Monochromator [5]. Before this device was operational, alternate methods were used to measure that quantity including absorption edges of Yttrium (Y) and Nickel (Ni). Fig. 9 shows an example of comparing the photon energy of the 3rd harmonic of the undulator radiation to the energy of the K absorption edge of the Yttrium component in the Ce:YAG screen. The left hand side diagrams show the Ce:YAG images of the LCLS x-ray pulse based on electron beams going through the undulator at different energies. The right hand side diagrams show differences of the left hand

side diagrams. X-ray wavelengths slightly above the Yttrium K absorption edge appear brighter in the images and stand out in the difference images; thus allowing a determination of the undulator *K* parameter.

The measurement confirms the CMM result for the undulator *K* value within a resolution of a few times 0.1% limited by our knowledge of the beam energy.

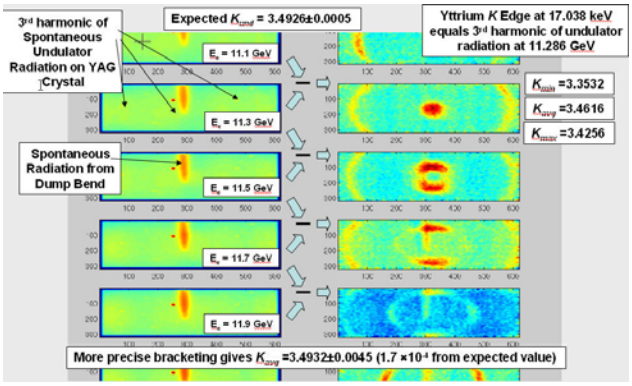

Figure 9: Ce:YAG images of the LCLS x-ray pulse based on electron beams going through the undulator at different energies.

BEAM-BASED ALIGNMENT

The electron beam trajectory through the FEL undulator must be straight to a level of about 2 µm over one FEL field gain length (~7 m).

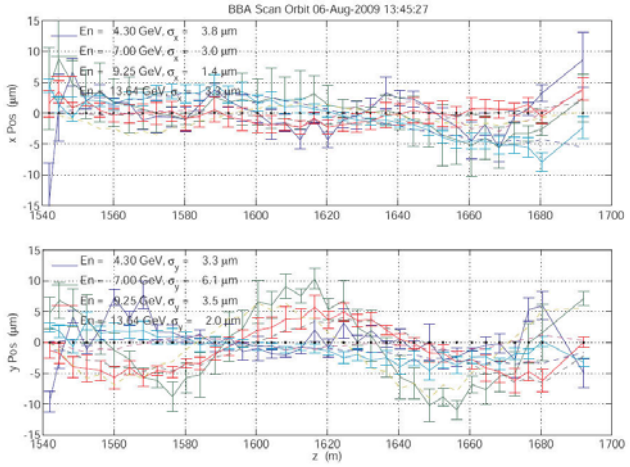

Figure 10: BBA Trajectories

This level is difficult to achieve using standard component survey methods. Instead, we use a special electron Beam-Based-Alignment (BBA) algorithm [6], which samples undulator BPM readings at four different beam energies. Changing the linac energy requires a change in many magnetic components upstream of the first undulator to keep the beam matched to the undulator optics, and to keep the horizontal and vertical position and angle of the trajectory at the entrance to the undulator independent of energy. A detailed description of this method has been published [6].

The BBA algorithm uses the off-axis field in the quadrupoles for trajectory correction. Changes are applied through cam-based girder motion, which will automatically align the quadrupoles in the process. Thus, the main source of the original trajectory errors, i.e., quadrupole misalignment, is taken out by BBA. Secondary sources, such as undulator field errors, the earth's magnetic fields, and other environmental fields are small and require slight off-center positioning of the quadrupoles to generate the required correction field on beam axis. The relative RFBPM position measurement resolution of <0.5 µm (rms) is sufficient to achieve trajectory straightness adequate to support 1.5-Å FEL operations.

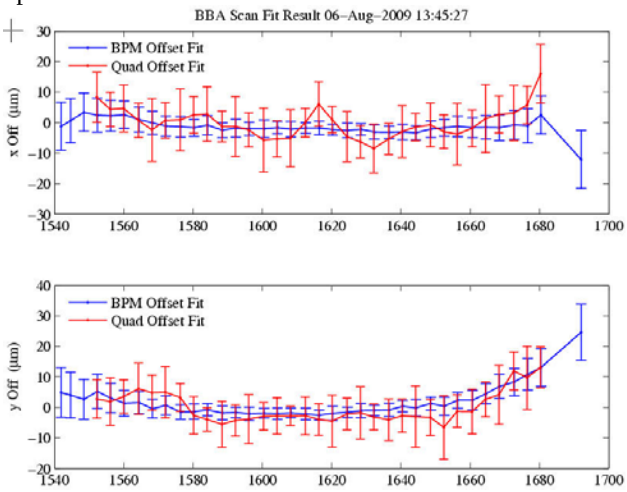

Figure 11: BBA Scan Fit Results

Fig. 10 shows the beam trajectories at 4 different energies (4.30 GeV, 7.00 GeV, 9.25 GeV, and 13.64 GeV) taken while only adjusting components upstream of but not along the undulator line. The algorithm turns out to be more successful than required and achieves rms trajectory straightness below 5 µm along the entire 132-m-long undulator line. The offset fits for quadrupole and BPM positions during a 4th BBA iteration is shown in Fig. 11.

BEAM FINDER WIRES

The Beam Finder Wire (BFW) device is a special wire scanner [7] with only two positions for the horizontal and vertical wire pair: The wires are either in a well reproducible "in"-position, in which they can be brought in collision with the electron beam, or in a "park"-position, where they won't affect the electron beam. The locations of the wires in the "in"-position have been fiducialized to tooling balls mounted on the device body and aligned to the undulator axis with high precision on the Coordinate Measurement Machine (CMM). Each BFW device enables control of the alignment of the girder at its up-stream end. After the upstream end of a girder has been aligned using BBA (see above), the downstream end can then be moved to bring the wires of the BFW device into collision with the beam, which completes the alignment of the girder, and thus the undulator segments relative to the beam axis. The BFW device provides a

means to accomplish a beam-based undulator segment alignment from the control room without the need for tunnel access. The BFW device is only needed for occasional verifications. The transverse position of the wires is monitored with the calibrated cam mover system. Local RFBPMs are used to measure and compensate for any shot-by-shot trajectory jitter during the scan.

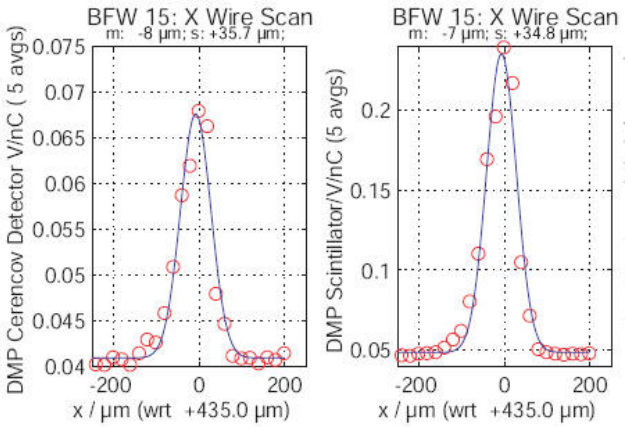

Figure 12: Results of a scan of the vertical (X-Wire) of BFW15 over a range of ±200 µm with 20-µm step size. Data points are the amplitudes of the scattered, reduced-energy electrons detected after they are bent by the dump magnets at a larger angle than the main electron beam.

Although not their primary purpose, the BFW wires also provide transverse beam profile and rms size information [8].

FIRST LASING

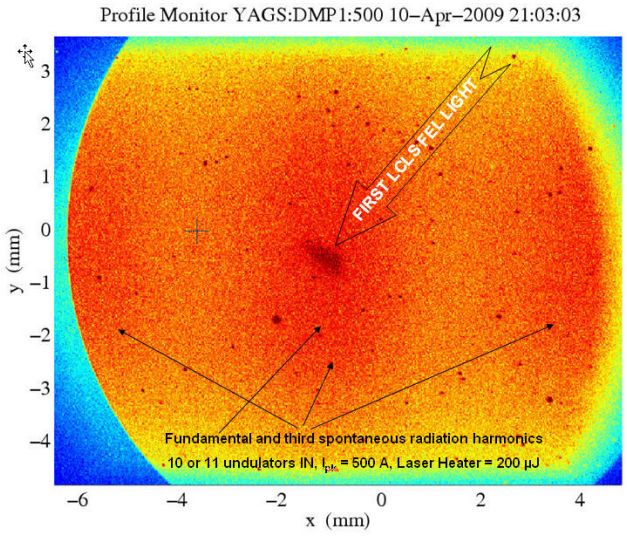

Figure 13: CE:YAG screen image of the X-Ray beam from a 13.64-GeV electron beam passing through 10 or 11 Undulator Segments. Visibile light has been prevented from reaching the screen by a thin Be foil)

First lasing occurred the first time more than 8-10 Undulator Segments were inserted while the electron beam was passing through the undulator vacuum chamber at an energy of 13.64 GeV and a bunch charge of 250 pC. Fig. 13 shows the first indication of the FEL signal at a much smaller divergence than the spontaneous synchrotron radiation that can be seen as a background (3rd harmonic dominant, fundamental superimposed on the 3rd harmonic, difficult to distinguish).

The FEL signal can be clearly distinguished even though FEL gain was actively suppressed at that point by running at low peak current (500 A) and large energy spread generated by the laser heater operating at 500 µJ).

After the peak current was brought to its design value of 3 kA (by compressing the bunch to a length of about 7 µm (rms)) and the laser heater was reduced to keep the slice energy spread at the design level of 0.01%, FEL saturation occurred after 14 Undulator Segments and the power gain length was measured at below 4 m. The measured gain length is significantly shorter than expected based on the goal slice emittance of 1.2 µm but compatible with the slice emittance of about 0.5 µm measured at the injector.

TAPERING

Adjusting the *K* values of the LCLS Undulator Segments by remotely controlling the *x* positions of the Undulator Segments is called tapering. The effective *K* stays constant throughout each Segment. Tapering is done as a stepwise change of *K* from Segment to Segment (segment tapering).

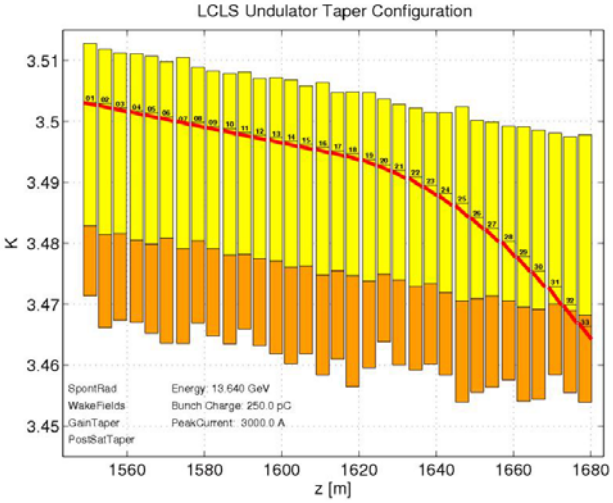

Figure 14: The yellow rectangles show the taper range (+6 mm > *x* > -5 mm) that is full supported by magnetic measurements for each of the 33 Undulator Segments. The orange boxes add extrapolated range for increased post saturation options. The red line shows the requested taper function, while the black bars represent the measured *K* values.

Tapering is essential for getting optimum FEL gain as electron beam parameters such as energy, peak current and bunch charge are changed. Tapering is normally done for four reasons: (1) to keep undulators tuned in the presence of energy loss from spontaneous synchrotron radiation depending on beam energy, (2) to compensate

for energy losses from longitudinal wakefields averaged over the core of the bunch depending on peak current and bunch charge, (3) to increase gain in the linear regime by slightly over-compensating, and (4) to add a strong taper after the saturation point to increase output power by factors of 2 to 4 [9].

Fig. 14 shows a typical taper configuration used at 13.64 GeV. The quadratic post-saturation taper has been determined experimentally.

RADIATION DOSES

The charged particle beam can produce various kinds of ionizing radiation at high levels if not properly controlled. Radiation damage to undulator magnets and electronics components installed inside the Undulator Hall has been of great concern during the design process. To control, i.e., minimize radiation damage a large number of monitoring devices (Beam Loss Monitors (BLMs), Beam Loss Fibers (BLFs), Comparator Toroids, Thermo-Luminescent Dosimeters (TLDs) and Machine Protection System (MPS) interlocks have been implemented.

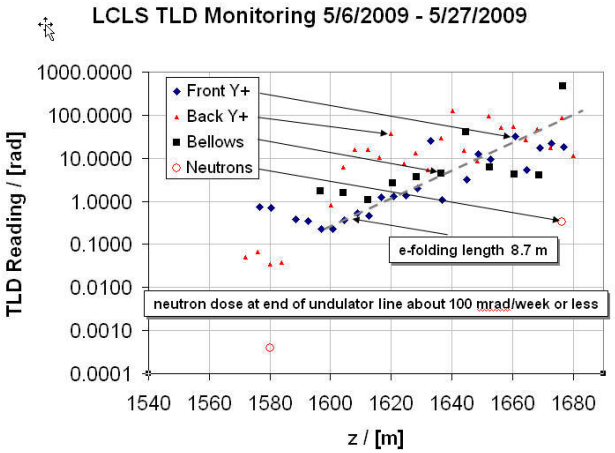

Figure 15: Shown are readouts of TLDs that had been placed inside the LCLS Undulator Hall over a period of 3 weeks as part of an on-going monitoring program. Four types of placement locations are show: entrance (blue diamonds) and exit (red dots) of the Undulator Segments, just above the beam-pipe, on top of the bellows, which is in closer proximity to the beam (black squares), and on top of the girders (inside moderators, only on girders 8 and 33).

The machine protection logic not only responds to various loss monitors but also to the electron beam trajectory inside the undulator vacuum chamber. It also prevents beam operation when screens or wires are inserted or removed from the beam. As a result, the measured radiation levels are low. Fig. 15 shows readouts from TLDs placed inside the Undulator Hall near Undulator Segments over a duration of 3 weeks while Undulators 8 to 33 were installed but girders 1 to 7 were still empty. The exponentially rising radiation levels appear to consist predominantly of low energy spontaneous synchrotron radiation, which is enhanced through the bunching that increases exponentially during the FEL process. Their energy appears to be too low to produce significant amounts of neutrons and thus too low to produce significant magnet damage. Before the regular installation of undulators, a first undulator was installed on girder 16 for a period of about 3 weeks. The 10 TLDs mounted around that device were changed on a weekly basis and showed about 100 mRad/week. This is in agreement with the levels shown at the 1600-m-position in Fig. 15 and appears to be due to higher energy radiation originating at the upstream tune-up dump/collimator or from further upstream. The undulator was measured magnetically after removal and found to be unchanged.

BEAM BASED TOLERANCE CHECK

During the design phase of the LCLS Undulator system, the sensitivity of the FEL process to several undulator parameters had been established with GENESIS simulations as part of a tolerance analysis.

Table 1: LCLS Undulator Tolerance Budget.

Parameter	σ_i[10]	f_i	$\sigma_i f_i$	Units
	@z_{end}	75%		
Optics Mismatch*	0.71	0.452	0.32	
Launch Error	30	0.186	3.7	μm
$\Delta K/K$	0.06	0.400	0.024	%
Segment x	1121	0.77	140	μm
Segment y	268	0.77	80	μm
Quad Gradient	8.8	0.029	0.25	%
Quad Position	4.7	.214	1.0	μm
Break Length	20.3	0.049	1.0	mm

Table 1 lists the result of the tolerance analysis with Fractions (f_i) of the fit parameter (σ_i) selected such that $e^{-\frac{1}{2}\sum f_i^2} = P/P_0 = 0.75$. P and P_0 are the FEL power levels for parameters at full tolerance level and for the error-free case, respectively. Some of these tolerances, i.e., horizontal segment placement, x_{UND}, undulator parameter, K_{eff}, and quadrupole gradient, k_{QUAD}, have been verified using the LCLS beam. In both situations, i.e., in simulation as well as with the actual electron beam, tolerances have been obtained based on random parameter distributions. For instance to determine the sensitivity of the FEL output to a given rms tolerance value, $\langle \Delta K \rangle_{rms}$, of the undulator parameter, 33 numbers, ΔK_i, were randomly selected to form a flat-top distribution in the range $K_{eff} \pm \sqrt{3}\langle \Delta K \rangle_{rms}$. The horizontal position of each undulator was then changed to detune by ΔK_i and the FEL intensity was measured. The measurement of the FEL intensity was either at the end of the undulator, i.e., after saturation or at a fixed point along the undulator, i.e., the saturation point of the undisturbed device.

* Defined via Twiss parameters as $\sqrt{(\beta\gamma_0 - 2\alpha\alpha_0 + \gamma\beta_0)/2 - 1}$

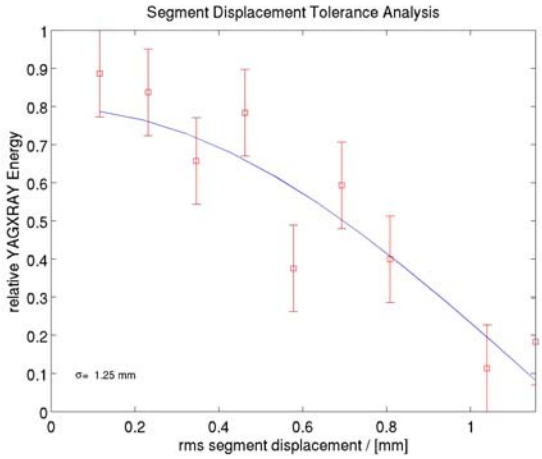

Figure 16: Relative FEL intensity after the last Undulator Segment extracted from the Ce:YAG screen as a function of random horizontal Undulator Segment positioning errors.

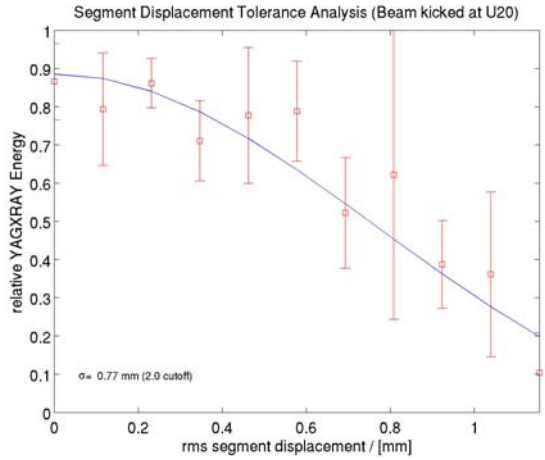

Figure 17: Relative FEL intensity at the 80-m location extracted from the Ce:YAG screen as a function of random horizontal Undulator Segment positioning errors.

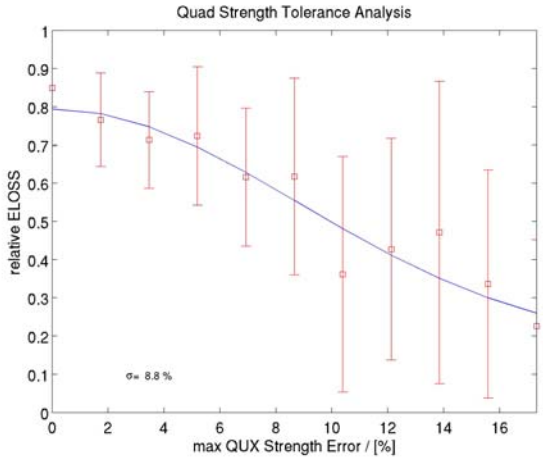

Figure 19: Relative FEL intensity after the last Undulator Segment extracted from average FEL electron energy loss as a function of random quadrupole gradient errors.

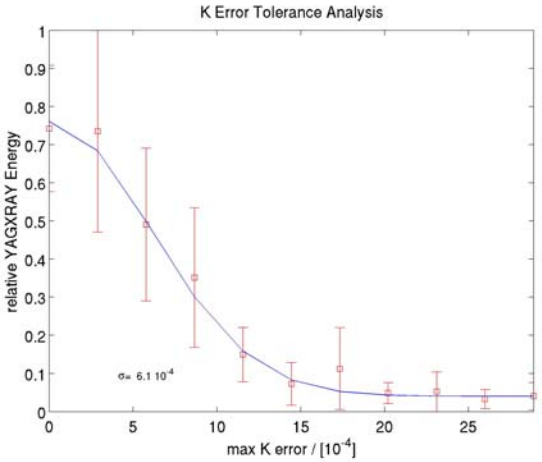

Figure 18: Relative FEL intensity after the last Undulator Segment extracted from the Ce:YAG screen as a function of random *K* errors.

In the beam-based analysis, several distributions for the same rms parameter value were generated to study the dependence on the random seed value. Figs. 16, 17, 18, and 19 show some of the results. The error bars are the rms values of the distributions of the results for different random seeds. The vertical axes are in arbitrary units. The solid lines in the figures show the result of Gaussian fits to the data.

Table 2: List of tolerance confirmed through the Beam Based method (BB) and comparison to result from GENESIS simulations shown in Table 1 (except for the first) (design).

Parameter	FEL to	σ (BB)	σ (design)
Segment *x*	$z_{sat.0}$	0.77 mm	0.78 mm
Segment *x*	z_{end}	1.2 mm	1.1 mm
K	z_{end}	6×10^{-4}	6×10^{-4}
Quad Strength	z_{end}	8.8%	8.8%

The fit results, i.e. the rms of the Gaussian, σ, listed in the lower left part of the figure, are summarized in Table 2 and compared with the design values. The beam based measurements are in very good agreement with the design simulations.

SUMMARY

The LCLS undulator system was successfully taken through commissioning and is now delivering X-ray FEL pulses to user experiments. The commissioning and FEL performance turned out better than expected. The X-ray FEL demands very tight tolerances on undulator segment alignment. These tolerances have been met through BBA procedures based on RFBPMs and quadrupoles (with energy scan) as well as BFW devices.

An Alignment Diagnostics System measures and enables the correction of girder movement due to ground motion, temperature changes, and cam mover changes. The monitor systems and the controls have been used

successfully for establishing and maintaining a straight FEL trajectory.

A number of component alignment tolerances have been verified using a beam-based method and found to be accurate.

ACKNOWLEDGEMENTS

It is a pleasure to acknowledge contributions by Argonne National Laboratory's LCLS team.

REFERENCE

[1] H.-D. Nuhn, P.J. Emma, G.L. Gassner, C.M. LeCocq, F. Peters, R.E. Ruland , "Electron Beam Alignment Strategy in the LCLS Undulators." FEL06 Proceedings, 529-536, SLAC-PUB-12098

[2] I. Vasserman, R. Dejus, P. Den Hartog, E. Moog, S. Sasaki, E. Trakhtenberg, and M. White, "LCLS Undulator Design Development." *FEL2004 Proceeding*, 2004.

[3] Z. Wolf, V. Kaplounenko, Y. Levashov, A. Weidemann, "LCLS undulator tuning and fiducialization," *In the Proceedings of Particle Accelerator Conference (PAC 07)*, Albuquerque, New Mexico, 25-29 Jun 2007, p 1320.

[4] J. Welch, "Air Temperature in the Undulator Hall." LCLS-TN-06-2, 2006.

[5] J. Welch et al., "Undulator K-Parameter Measurements at LCLS." This conference

[6] Emma P., Carr R., Nuhn H.-D.," Beam-Based Alignment for the LCLS FEL Undulator," NIM-A vol. 429, no 1-3, pp. 407-413, ISSN 0168-9002 (1999).

[7] J. Wu, P. Emma and R.C. Field, "Preliminary Study on Electron Signal Detection for the Beam Finder Wire of the LCLS Undulator." LCLS-TN-06-7, 2006.

[8] J. Welch, "Estimate of Undulator Magnet Damage Due to Beam Finder Wire Measurements." LCLS-TN-06-6, 2006.

[9] WM.Fawley, Z. Huang, K-J. Kim, N.A. Vinokurov, "Tapered undulators for SASE FELs," NIM-A, vol 483, (1-2), pp 537-541 (2002)

[10] Derived by S. Reiche through FEL simulations using his FEL simulation code, GENESIS 1.3.

.